Published in final edited form as:
J Mol Biol. 2007 November 23; 374(2): 487–499. doi:10.1016/j.jmb.2007.09.035.

R-subunit Isoform Specificity in Protein Kinase A: Distinct Features of Protein Interfaces in PKA Types I and II by Amide H/^{2}H exchange Mass Spectrometry

Ganesh S. Anand[4,1,+], **Matthew Hotchko**[2,3,+], **Simon H.J. Brown**[2], **Lynn F. Ten Eyck**[2,3], **Elizabeth A. Komives**[2], and **Susan S. Taylor**[2,4,**]

[2] Department of Chemistry and Biochemistry, University of California, San Diego, La Jolla, CA 92093-0378, USA

[3] San Diego Supercomputer Center, University of California, San Diego, 9500 Gilman Drive, La Jolla, CA 92093-0505, USA

[4] Howard Hughes Medical Institute, University of California, San Diego, 9500 Gilman Drive, La Jolla, CA 92093-0359, USA

Abstract

The two isoforms (RI and RII) of the regulatory (R) subunit of cAMP-dependent protein kinase or protein kinase A (PKA) are similar in sequence yet have different biochemical properties and physiological functions. To further understand the molecular basis for R-isoform-specificity, the interactions of the RIIβ isoform with the PKA catalytic (C) subunit were analyzed by amide H/^{2}H exchange mass spectrometry to compare solvent accessibility of RIIβ and the C subunit in their free and complexed states. Direct mapping of the RIIβ-C interface revealed important differences between the intersubunit interfaces in the type I and type II holoenzyme complexes. These differences are seen in both the R-subunits as well as the C-subunit. Unlike the type I isoform, the type II isoform complexes require both cAMP-binding domains, and ATP is not obligatory for high affinity interactions with the C-subunit. Surprisingly, the C-subunit mediates distinct, overlapping surfaces of interaction with the two R-isoforms despite a strong homology in sequence and similarity in domain organization. Identification of a remote allosteric site on the C-subunit that is essential for interactions with RII, but not RI subunits, further highlights the considerable diversity in interfaces found in higher order protein complexes mediated by the C-subunit of PKA.

Keywords

amide H/^{2}H exchange; MALDI-TOF; protein kinase A; RIIβ isoform; cAMP signaling

The adenosine 3′, 5′ cyclic monophosphate (cAMP) signaling pathway plays a critical role in the cell, serving to transduce the action of a wide variety of hormonal stimuli across

**Corresponding author: Susan S. Taylor Ph.D., Howard Hughes Medical Institute, University of California, San Diego, La Jolla, CA 92093. (858) 534-8193 (fax), staylor@ucsd.edu.
[1]Present Address: Department of Biological Sciences, National University of Singapore
+These authors contributed equally to this work.

species ranging from bacteria to mammals [1]. In most eukaryotic cells, cAMP exerts a broad influence inside the cell primarily through its activation of Protein Kinase A (PKA), a key enzyme with numerous intracellular substrates [2]. PKA is a master switch that controls a wide range of cellular functions which are in turn regulated by cAMP. In the absence of cAMP, PKA exists in an inactive state as a tetrameric holoenzyme composed of a homodimeric regulatory (R) subunit and two catalytic (C) subunits. Binding of cAMP leads to dissociation of the holoenzyme to unleash the active C subunit. The R-subunit is thus a primary locus for cAMP in the cell. By toggling between C-subunit bound and cAMP-bound states, the R-subunit functions as a cAMP-dependent regulator of PKA phosphotransferase activity [3].

There are two principal isoforms of the R-subunit (type I and type II) [4] each further sub classified into α and β subtypes. R-subunits are highly modular with an N-terminal dimerization/docking domain (D/D domain) joined by a variable linker to two cAMP binding domains (Domain A and B) (Figure 1A). The linker region contains a PKA phosphorylation consensus motif which serves as a docking site for the C-subunit and can be considered the primary C-subunit recognition site (RS1). Differences in primary sequence within this motif distinguish the two isoforms of the R-subunit. In the RI isoforms, the site of phosphorylation is substituted by an alanine or glycine making this segment a pseudosubstrate inhibitor while in the RII isoforms, this site is a serine that is phosphorylated by PKA and functions as a substrate inhibitor of PKA [4]. Sequence alignments of mammalian RIα and RIIβ show high homology (> 60% sequence identity) within the cAMP-binding domains but variability within the D/D domain and linker [5]. Despite high sequence similarities and a similar domain organization, the R-subunit isoforms show major differences in their subcellular localization and physiological function [6–10]. The molecular basis for the dramatic differences in physiology and function of the two R-subunit isoforms are not yet completely understood. One approach to understanding the molecular basis for isoform specificity has been to characterize the unique non overlapping protein-protein interactions mediated by the R-subunits with two important protein partners:- A-Kinase Anchoring Proteins (AKAPs) and the PKA C-subunit. In this study we have focused on interactions of the RIIβ isoform with the C-subunit.

Deletion mutagenesis of the R-subunit has been successfully used to map its interactions with the C-subunit. The D/D domain which is the binding site for AKAPs is not required for high affinity holoenzyme complex formation [11]. Studies first carried out with the RIα isoform, revealed a multivalent mode for binding of the R-subunit with the C-subunit, requiring interactions at more than one site to achieve high-affinity binding (K_D= 0.2nM) [11–13]. These sites included the pseudosubstrate, primary interaction site [14] and a second site within the cAMP-binding domains which together confer high affinity binding for the C-subunit [11]. Complementary amide H/^{2}H exchange mass spectrometry [15] and X-ray crystallographic analyses of the RIα-C complex [16] have provided detailed descriptions of the RIα-C interface. amide H/^{2}H exchange MS revealed decreased exchange in RIα at both the pseudosubstrate site and a peripheral recognition site within Domain A [15] and at the active site cleft and C-lobe of the C-subunit in the RIα-C complex. These sites were subsequently confirmed in the crystal structure of the RIα-C complex [16].

Previous amide exchange studies on the full length RIIβ isoform mapped differences in exchange between RIIβ, free in solution and in complex with the C-subunit [17]. However, for a detailed mapping of the interface it is necessary to also identify the interface contributed by the C-subunit. In this study, we have used deletion mutagenesis to localize interactions of different regions of RIIβ to C-subunit amide H/^{2}H exchange MS to map interfaces of complexes of the C-subunit with different deletion fragments of RIIβ. We have also tested the effects of Mg^{2+}ATP on the RIIβ-C complex. Our results have revealed

important differences in the intersubunit interface between the RIα and RIIβ holoenzyme complexes and provide new insights into isoform-specificity in PKA

Results

Deletion mutagenesis of RIIβ and contribution of cAMP binding domain:A to high affinity interactions with the C-subunit

Following earlier work on RIα [11], we initially engineered a deletion mutant of RIIβ, spanning the primary C-subunit interaction site and Domain A and tested its ability to bind the C-subunit. This mutant, RIIβ(108–268) (Figure 1B) is analogous to RIα(91–244) which binds the C-subunit with high affinity in the presence of Mg^{2+} ATP [11]. Since the γ-phosphate is transferred to the substrate site in the Mg^{2+}ATP-bound RIIβ:C holoenzyme complex [18], we replaced Mg^{2+}ATP with the nonhydrolyzable analog, adenylylimidodiphosphate in the presence of $MnCl_2$ (Mn^{2+}AMP-PNP). This analog mimics ATP with a nitrogen substitution at the oxygen connecting the β and γ-phosphate groups and is an excellent analog to study active conformations of kinases because of its ability to trap kinases in their transition states and has thus been very useful in studying PKA [16,19]. To test binding of the RIIβ deletion mutant with the C-subunit, surface plasmon resonance (SPR-Biacore) was used. RIIβ(108–268) in the presence of Mn^{2+} and AMP-PNP binds the C subunit with significant affinity (K_D = 12.0 nM) (Table 1) but this is approximately 60-fold less than the affinity of RIα(91–244) (K_D = 0.2 nM in the presence of Mg^{2+}ATP) [20] or full-length RIIβ(K_D = 0.6 nM) [21]. Interestingly, in the absence of Mn^{2+} and AMP-PNP, no binding of RIIβ(108–268) to the C-subunit was observed in SPR-Biacore as well as gel filtration chromatography (Brown, S.H.J. and Taylor, S.S., unpublished observations).

Solvent accessibility changes in RIIβ and C-subunits by amide exchange mass spectrometry

We next set out to measure solvent accessibility by amide H/^{2}H exchange MS in the free C-subunit and in complex with the different engineered deletion mutants of RIIβ Our analysis was primarily targeted to the C-subunit and included only a limited number of peptides from the RIIβ subunit since changes in RIIβ upon complexation with the C-subunit by amide exchange mass spectrometry have been characterized previously [17]. These earlier studies identified a single peptide spanning residues 253-268, from among 38 peptides of RIIβ analyzed, that showed decreased exchange in the RIIβ:C complex under similar experimental conditions (Figure 1C). We included seven peptides from RIIβ(108–402) covering 28% of the sequence and two peptides from RIIβ(108–268) covering 19% of the sequence in our analysis. Both sets included the critical C-interface peptide RIIβ253–268). Amide H/^{2}H exchange experiments were carried out over a five minute period at 23 ± 1°C by preparing 10-X fold dilutions of protein samples in deuterated buffer (5 μl of protein solution with 45 μl of deuterated buffer (50 mM MOPS, 50 mM NaCl, 1 mM DTT pH_{read} 7.0)), followed by “on-exchange” incubation for varying times (0 – 5min)) prior to quenching in 0.2% TFA, pH 2.5 at 0 °C followed by pepsin digestion. Mass spectrometry data were analyzed and the average numbers of deuterons were calculated as described in Materials and Methods. Fourteen peptides from the C-subunit could be analyzed from all of the samples, and these covered nearly 40% of the sequence of the C-subunit similar to coverage studied in previous studies on the RIα:C complex [22]. Centroids were calculated from the mass envelopes that had the natural abundance isotope profiles removed by deconvolution. This method was shown in previous studies to increase sensitivity and accuracy by removal of stochastic widening and by noise reduction due to local averaging [23]. The software package DEX was used for both the deconvolution and centroid calculations. The average number of deuterons (Ds) exchanged (2 min) for each peptide is given in Table 2. For those segments where changes were observed, plots of the time-course

of deuteration are also shown and either computing the average exchange at the 2 min time point or calculating the exchange rate from the plot results in the same conclusions [24]. Extending the time-course of the experiment also did not result in observation of any further differences. In comparing the average numbers of deuterons exchanged between samples, only differences in exchange greater than 1 Da have been interpreted to be significant. Exchange after two min. of deuteration for one peptide each from RIIβ(*m/z* = 2281.31) and the C-subunit (*m/z* = 1793.97), residues 247–261 are shown in figures 2 and 3 respectively.

Except for two overlapping peptides, C8, C(163–172) and C9, C(164–174), no solvent protection was seen in any of the other C-subunit peptides in the RIIβ(108–268):C complex in the presence of Mn^{2+} AMP-PNP compared to the C-subunit bound to Mg^{2+} ATP (Table 2). There was also no solvent protection in any of the RIIβ peptides analyzed in the RIIβ(108–268):C complex plus Mn^{2+} AMP-PNP (Table 2).

Contribution of cAMP binding domain:B to high affinity interactions with the C-subunit

The observed weak binding of RIIβ(108–268) to the C-subunit suggested that Domain B might be important for high-affinity interactions with the C-subunit. To test this, we characterized the complex formed by the C-subunit and a larger fragment of RIIβ, spanning both cAMP binding domains. However, because the C-terminal residues of RIIβ(403–416) are susceptible to proteolytic cleavage during purification of the holoenzyme, it was necessary to use a slightly truncated construct RIIβ(108–402). The resulting truncated protein was very stable and retained all of the properties of the larger construct including C-subunit and cAMP binding (Brown, S.H.J. and Taylor, S.S., unpublished observations). Biacore-SPR analysis revealed that the RIIβ(108–402) construct alone binds with higher affinity to the C-subunit unlike the shorter construct containing Domain A alone. Mn^{2+} AMP-PNP further enhances interactions with the C-subunit (Table 1).

Amide $H/^{2}H$ exchange analysis showed that within a single region of RIIβ(108–402) spanning residues 253-268 (m/z=2281.31) (Figure 1C), nearly ten amides were protected from solvent in the RIIβ(108–402)-C holoenzyme complex (after 2 min deuteration (Figure 2 and Table 2). Interestingly, most of the other peptides analyzed, including peptide 354–371 that spans the cAMP binding site of Domain B in RIIβ showed increased exchange in the holoenzyme complex. This is consistent with previous studies on the full-length RIIβ:C complex that showed this is the only region in full-length RIIβ that showed decreased exchange under similar short timescale deuterium ‘on exchange’ conditions [17]. This is also consistent with earlier studies describing allosteric communication between the C-subunit and cAMP-binding sites in RIα [15].

All peptides with the exception of the α:C helix spanning peptides C5, C(92–100), and C1, C(27–40) both within the N-lobe of the C-subunit showed protection in the RIIβ(108–402):C (+Mn^{2+} AMPPNP) complex relative to the C-subunit bound to Mg^{2+}ATP (Figure 4, Table 2). The peptide, C(44–54) corresponding to the glycine-rich loop showed solvent protection (~ two amides) in the RIIβ(108–402):C complex (4A). This protection seen was localized to ~one amide protection each within residues 41–44 and 45–54 through subtractive analysis using exchange data from a larger, overlapping fragment, C3, C(41–54) (Table 2). These results suggest that the Domain B somehow enhances binding of the substrate/product inhibitor region of RIIβ(108–112) to the active site cleft of the C-subunit. The C-subunit residues 163-172 corresponding to the catalytic loop were completely shielded from solvent in both RIIβ(108–268)• C-subunit and RIIβ(108–402)•C-subunit complexes (Figure 4B). The protection (one amide after 2 min.) for both complexes presumably reflects locking-in of the Mn^{2+}AMP-PNP in the active site of the C-subunit, completely burying these residues from solvent. Results of amide exchange in the three C-lobe peptides of the C-subunit are shown in Figure 5. There were no significant differences

in exchange between the free C-subunit and RIIβ(108–402) complexes within residues 212-221 corresponding to the APE-α:F loop (5A). Decreased exchange was observed in the α:G helix C(247–261) (Figure 5B) (2 amides protected after 2 min. exchange) in the RIIβ(108–402):C complex. The C-subunit residues 278-289, corresponding to the α:H-α:I loop, also showed a significant decrease in solvent accessibility when RIIβ(108–402) was bound (Figure 5C).

Role of ATP in holoenzyme complex formation

To examine the effects of Mg^{2+}ATP on RIIβ interactions with the C-subunit, we compared the RIIβ•C binding kinetics and amide exchange of the RIIβ(108–402)•C-subunit complex in the presence and absence of Mn^{2+}AMP-PNP. A relatively small (~8-fold) increase in RIIβ•C-subunit binding affinity was observed in the presence of Mn^{2+}AMP-PNP (Table 1).

Two of the N-lobe peptides (C4, C(66–83) and C5, C(92–100)) showed increased exchange while the Glycine-rich loop peptide C3, C(41–54) showed decreased exchange in the RIIβ(108–402):C complex-bound to Mn^{2+}AMP-PNP compared to the RIIβ(108–402):C apo complex. There were no significant differences in amide H/^{2}H exchange between the two complexes in three C-lobe peptides (C10, C11 and C12 in Table 2) of the C-subunit that are part of the RS2 interaction interface. This is consistent with Mg^{2+}ATP not being obligatory for high-affinity RIIβ:C interactions [21]. Residues 163-172, corresponding to the catalytic loop, were completely protected whether Mn^{2+}AMP-PNP was present or not in the RIIβ(108–402):C complex.

Comparison of RIα and RIIβ complexes with the C-subunit in the presence of Mn^{2+}AMP-PNP

Comparison of amide exchange (2 min. deuteration) in the C-subunit bound to Mg^{2+}ATP, the C-subunit in complex with RIIβ(108–402) plus Mn^{2+}AMP-PNP and the C-subunit in complex with full-length RIα plus Mg^{2+}ATP revealed many differences between the two isoforms (Figure 7). While all peptides showed decreased solvent accessibility upon complex formation, the extent of protection observed varied widely in the two complexes. Two of the C-lobe peptides showed more protection for the RIIβ(108–402) complex than the full-length $RI\alpha_2$•C_2 complex. After deuteration for 2 min, close to three amides were solvent protected in C-subunit residues 278-289 in the RIIβ(108–402) complex, while only one amide showed protection in the $RI\alpha_2$•C_2 (Figure 7A). More than two amides were protected in C-subunit residues 247-261 in the RIIβ(108–402) complex, while roughly one amide showed protection in the $RI\alpha_2$•C_2 complex (Figure 7B).

Within the N-lobe of the C-subunit, residues 163-172 and residues 133-145 showed no differences in exchange between the two complexes (Figure 7D, E). However, the glycine rich loop represented by C-subunit residues 44-54 revealed significant differences between the two complexes. This region of the C-subunit showed no significant protection in the RIIβ complex in contrast to the RIα complex (~2D) (Figure 7F). The results indicate an inverted pattern of solvent protection between the RIα and RIIβ complexes. In the RIIβ complex, the C-lobe residues 212-221 showed almost no changes in the RII complex in contrast to the large protection in the RI complex, while the glycine-rich loop showed the opposite with a greater protection in the RIα complex.

Discussion

R-subunit isoform differences in holoenzyme complexes: Unique importance of cAMP:B domain in RIIβ

A critical aspect in PKA research is the existence of nonredundant R-subunit isoforms that show major differences in tissue specificity, subcellular localization and function and, consequently, have distinct physiological functions despite having similar domain organization and conserved cAMP-binding domains [25]. Extensive deletion mutagenesis [11] and structural studies on the RIα complex with the C-subunit [16] have provided detailed information on the R-C intersubunit interface. These reveal multivalent modes of binding of RIα to the C-subunit using the pseudosubstrate/inhibitor site or recognition site 1 (RS1), and the cAMP-binding domains contributing the peripheral interaction site or recognition site 2 (RS2) for binding C-subunit. These studies also showed that Domain A contributed the bulk of the RIα:C interface and showed nearly identical binding affinity as reported for the full-length complex [13], [20]. In RIα the α:A and α:C helices contributed to interface formation [26], later confirmed by X-ray crystallography [16], whereas in RIIβ, only one peptide (residues 253-268) spanning helix α:C (Figure 1C) showed decreased solvent accessibility in the full-length RIIβ-C complex [17], reconfirmed in the present study with deletion mutants of RIIβ. Small angle X- ray scattering [27] and protein footprinting studies [28] have previously hinted at differences in overall shapes of the R subunit type I and type II PKA complexes.

Here we show that in contrast to RIα, the binding of RIIβ to C critically depends on the presence of Domain B. This domain enhances the binding affinity by 40–60-fold and is not ATP-dependent. Furthermore, despite high sequence conservation between RIα(91–244) and RIIβ(108–268), the RIIβ(108–268):C complex in the presence of AMP-PNP is very different from the RIα(91–244):C complex. RIIβ(108–268) shows a rapid dissociation rate and lower affinity for the C-subunit compared to RIα(91–244) while amide exchange revealed several regions in the C-lobe of the C-subunit that are associated with decreased exchange in the RIα(91–244):C complex but are unaffected when complexed to RIIβ(108–268) under identical experimental conditions with the same sequence coverage and peptides analyzed. Based on the H/D exchange data alone, it is unclear how Domain B contributes to RIIβ:C interactions. Absence of solvent protection in the C-terminal peptide in the RIIβ(108–268):C(+Mn^{2+} AMP-PNP), R2, RIIβ(253–268) relative to the RIIβ; (108–402):C(+Mn^{2+} AMP-PNP) suggests that the C-terminus in RIIβ(108–268) and RIIβ(108–268):C(+Mn^{2+} AMP-PNP)might be disordered and consequently shows a weaker affinity for binding the C-subunit. Domain B might facilitate direct interactions with the C-subunit either through direct interface contacts between Domain B, RIIβ(269–402) and the C-subunit. Alternatively, RS2 might still be contributed entirely by Domain A but unlike in RIα, Domain B might be required for proper folding of Domain A. X-ray crystallographic analyses of RIIβ(108–268):C(+Mn^{2+} AMP-PNP) show that the α:C helix, RIIβ(253–268) is ordered and mediates direct interactions with the C-subunit (Brown, S.H.J. and Taylor, S.S., unpublished results). However the ordering might be a consequence of crystal packing and ordering as the α:C helix, RIIβ(253–268), in the absence of Domain B is disordered in solution from our results. A direct role for Domain B in mediating direct interactions with the C-subunit is evident from X-ray crystallography on a deletion mutant of RIIβ containing both cAMP-binding domains (Wu, J., Brown, S.H.J., von Daake, S. and Taylor, S.S. (2007), *Science* in press). In this structure, Domain B has been found to mediate direct interactions with the αHαI loop of the C-subunit. It is not clear if there are similar direct interactions between Domain B of RIIβ and C-subunit since amide H/^{2}H exchange studies on the full-length RIIβ:C complex showed no regions of significant solvent protection in Domain B [17]. It is therefore possible there are different roles for Domain B in RIIβ:C and RIIβ:C complexes.

Distinct, overlapping surfaces on the C-subunit mediate interactions with RIα and RIIβ

The results presented in this study reveal a clear difference between the binding of the C-subunit with the RI and RII isoforms. Previous amide H/^{2}H exchange studies on the RIα:C holoenzyme complex revealed large decreases in amide exchange in two surface segments of the C-subunit; residues 212-221 and 247–261. In addition, only a slight protection was observed in residues 278-289 when Domain B was present (full-length RIα) [22]. RIIβ binding also decreased solvent exchange in residues 247-261 but to a lesser extent than RIα (Figure 7). Greater protection was observed for residues 247-261 whereas no significant protection was observed for residues 212-221. In addition, when RIIβ(108–402) was bound to the C subunit, three fewer amides exchange within residues 278-289, whereas less than a single amide was protected for this region when in complex with RIα.

Allostery between residues 278-289 (C) and the active site of the C-subunit

Interestingly the peptide, 278–289 (Figure 5C) showed greater exchange in the RIIβ(108–268)•C complex than was observed for the C-subunit bound to Mg^{2+}ATP. This increase in exchange was observed concomitantly with decreased exchange in residues 163-172, an N-lobe fragment contributing to RS1 and spanning the catalytic loop of the kinase. Usually, we have interpreted such increases in exchange with long-range conformational effects as "allostery" although this term is not used in the traditional sense. In other words, binding of the RIIβ pseudosubstrate sequence and ATP at the active site subtly alters the conformation and/or dynamics of residues 278-289. The increase in exchange observed for RIIβ binding was not observed for RIα binding where the analogous truncated RIα(94–244) showed very weak protection that was only slightly greater for the full-length RIα [22]. In fact, this very weak protection was misinterpreted as interface protection causing a slight skew of the initial models proposed from H/^{2}H exchange and docking [29]. There is a greater protection in this region in the larger than RIIβ(108–402):C than observed for full-length RIα strongly suggesting that in the case of RIIβ, this region is a major contributor to the RS2 interface. These amide H/^{2}H exchange results therefore suggest that binding at RS1 is allosterically linked to binding at RS2 for the RIIβ subunit, but much less so for the RIα subunit.

These results are very consistent with parallel studies on kinases. Residues comprising the loop between αH and αI are unique to the AGC family of protein kinases (Figure 7G,H), and are thought to play a regulatory role in other cases as well [30]. Mutagenesis has also highlighted allosteric cross-talk between the active site and the αH-αI loop. Amide H/^{2}H exchange studies have shown that a mutant Tyr204Ala that decreased catalytic rates of phosphotransfer rate showed increased exchange in three peptides in the C-terminal lobe including the αH–αI loop indicating long range allosteric networks coupling the active sites with this region [31]. Conversely, a mutation in this loop Lys285Pro were isolated in a screen that rescued catalytically defective mutations in the yeast homolog of PKA and this mutant protein blocked interactions with the RII subunit but not RI highlighting both the importance of this region in interactions with the RII subunit in addition to being important for allosteric networks in the kinase (Yang, J. and Taylor, S.S., manuscript in preparation). The importance of this region in recognition of protein substrates has been highlighted by a novel genetic approach for identifying PKA substrates in *Saccharomyces cerevisiae* [32]. In this study the region on the kinase spanning the αH–αI loop was a secondary site for substrate recognition.

ATP is not obligatory for formation of high-affinity RIIβ-C holoenzyme complexes

ATP and 2 Mg^{2+} ions are required for formation of a high-affinity RIα •C complex. In its absence, the K_D for R-C interactions is approximately 100-X fold weaker [33]. A primary classification of the R-subunits into RI and RII isoforms is based on the ability to accept the γ-phosphate at its PKA at the pseudosubstrate/autoinhibitor site or RS1. RIα contains an

inhibitor sequence that can not be phosphorylated while RIIβ contains a pseudosubstrate sequence that is phosphorylated [4]. Thus, it was a surprise that the RIIβ subunit appeared to bind with similar affinity whether or not the ATP analog was present, and tight binding depended mostly on the presence of the cAMP-binding B-domain. When only the cAMP-binding Domain A was present, protection of RS1 residues 44-54, 133-145, and 163-172 is not seen (Table 2). This is most likely due to the rapid dissociation of the truncated RIIβ(108–268) mutant. When both cAMP-binding domains were present, the protection observed at RS1 was nearly identical in the presence and absence of ATP (Table 2). It is interesting to note, however, that even in the RIIβ(108–402)•C holoenzyme complex, the glycine-rich loop showed greater exchange than in the RIα•C holoenzyme complex (Figure 7). This reinforces the idea that the primary determinant for formation of a high affinity complex of RIα with the C-subunit is occupancy of the active site cleft by the pseudosubstrate site (RS1) whereas binding of RIIβ is dependent primarily on RS2 interactions require both cAMP-binding domains. Furthermore this binding is insensitive to the presence or absence of ATP reported previously [18]. It therefore appears that the ability to bind in the absence of ATP (by strong RS2 binding) allows RIIβ to regulate the C-subunit in low ATP environments such as adipose tissue [25].

In summary, mechanisms for PKA regulation mediated by RI and RII are very different. RIIβ requires both cAMP binding domains to interact with the C-subunit. This RS2 interface site in RIIβ complex might compensate for decreased interactions at RS1 to maintain a high-affinity complex even in the absence of ATP. This might explain the distinct differences in nature of C-subunit inhibition by the two R-subunit isoforms with the RI and RII functioning as competitive and noncompetitive inhibitors respectively [34]. Our results clearly indicate that the C-subunit of the kinase thus shows multiplicity in molecular interactions with different R-subunit isoforms and provides a basis for isoform-specificity in the PKA R-subunit.

Materials and Methods

Materials

ATP, cAMP, MOPS and cAMP immobilized on 6 % agarose were obtained from Sigma. Deuterium oxide, D_2O (99.9% deuterium) was obtained from Cambridge Isotopes.

Expression and purification

Proteins were expressed in *E. coli* BL21 (DE3) cells (Novagen) and purified as described previously using cAMP-agarose resin [35]. Following cell lysis, protein was precipitated from the soluble fraction by 60% saturated ammonium sulfate (AS) at 4 °C. The AS pellets were resuspended, incubated overnight with the cAMP-resin, and eluted at room temperature. For cAMP-bound RIIβ, the protein was eluted with buffer containing 25 mM cAMP. For cAMP-free RIIβ, the protein was eluted with buffer containing 25 mM cGMP. The protein eluates were then purified over a S75 gel filtration column to remove excess cGMP, in 50 mM MES, 200 mM NaCl, 2 mM EDTA, 2 mM EGTA, 10 mM DTT, pH 5.8 (buffer A). Proteins were concentrated with 10 kDa molecular weight cutoff Millipore concentrators prior to deuterium exchange (RIIβ(108–268) (45 μM), RIIβ(108–402)(75 μM)). The C-subunit was prepared as described [36] and concentrated to 75 μM prior to deuterium exchange experiments. The purified C-subunit (apo) was incubated with 50 mM MOPS, 50 mM NaCl, 1 mM DTT, 2 mM $MgCl_2$ and 0.2 mM ATP to prepare samples of C bound to ATP, concentrated to 125 μM prior to deuterium exchange experiments.

Holoenzyme formation

To prepare holoenzyme in the absence of ATP, cAMP-free RIIβ was added to wild-type C-subunit in a 1:1.2 molar ratio and dialyzed at 4 °C against 10 mM MOPS, 50 mM NaCl, 1mM EDTA, 2 mM DTT, pH 6.5 (buffer B). To prepare holoenzyme in the presence of ATP analog the same dialysis steps were followed with buffer B modified to include 1 mM $MnCl_2$ and 0.2 mM AMP-PNP (ATP analog) [16] (Buffer C). To remove excess C-subunit, the complex was purified by elution through a S200 gel filtration column and then concentrated with 30 kDa molecular weight cutoff Millipore concentrators (RIIβ(108–402):C complex (40 μM), RIIβ(108–402):C complex (50 μM)(+ Mn^{2+} AMP-PNP), RIIβ(108–268):C complex (75 μM)) prior to deuterium exchange and stored in buffer B or buffer C respectively at 4 °C.

Surface Plasmon Resonance

Surface plasmon resonance was used to measure the interaction kinetics of the C-subunit and RIIβ subunits using a Biacore 3000 instrument (GE Healthcare Life Sciences). The C-subunit was immobilized to a CM dextran surface sensor chip (Biosensor amine coupling kit). All binding interactions were performed at 25 °C in 20 mM MOPS, 150 mM KCl, 1 mM TCEP, pH 7.0, 0.005% polysorbate 20, pH 7.0 buffer. All AMP-PNP samples were done with .2mM AMP-PNP and 1mM $MnCl_2$. After injection of the R-subunit, the C-subunit surface was regenerated by injection of 1 min (25–50uL) μL of 30 μM cAMP in the running buffer. Kinetic constants were calculated using the Biacore pseudo-first order rate equation and affinity constants (K_D) were calculated from the equation $K_D = k_d/k_a$ [33].

Deuterium exchange experiments

Deuterated samples were prepared at 23 ± 1 °C by diluting 5 μl of protein solution with 45μl of deuterated buffer A(50 mM MOPS, 50 mM NaCl, 1 mM DTT pH_{read} 7.0), followed by “on-exchange” incubation for varying times (0 – 10min) prior to quenching in 0.2% TFA, pH 2.5 at 0 °C. The exchange mixtures for the C-subunit in the presence of Mg^{2+} and ATP included 2 mM $MgCl_2$ and 0.2 mM ATP with buffer A. The exchange mixture for the RIIβ(108–402):C and RIIβ(108–268):C complexes contained 2 mM $MnCl_2$ and 0.2 mM AMP-PNP with buffer A. The quench buffer for free RIIβ(108–268), RIIβ(108–402) and RIIβ(108–402):C complex included 1 mM EDTA with buffer A. Deuterium exchange at time t = 0, was determined by adding the protein solution in H_2O (5 μl) to a mixture of 0.5 ml 0.1% TFA and deuterated buffer A (45 μl). A mock experiment was performed to determine the amount of 2% TFA required so that upon quenching, the pH would be 2.5. A portion of the quenched reaction (0.1 ml) was mixed with 50 μL of pepsin bead slurry (previously washed two times in 1 ml of cold 0.1% TFA). The mixture was incubated on ice with occasional mixing for 5 min, centrifuged for 15 s at 12,000 × g at 4°C, divided in aliquots, frozen in liquid N_2, and stored at −80°C until analyzed.

Frozen samples were quickly defrosted to 0°C, mixed with matrix (5 mg/ml a-cyano-4-hydroxycinnamic acid in 1:1:1acetonitrile, ethanol, 0.1% TFA, final pH 2.5, 0°C), and 1 μl was spotted on a chilled MALDI target. The target was quickly dried and analyzed on a Voyager DE STR Biospectrometry Workstation (Applied Biosystems Inc., Foster City, CA) as described in earlier studies [37].

Data analysis

Mass spectra were calibrated as described previously [15] and then converted to ASCII text for further analysis. The mass spectrometry data was analyzed using DEX software [23] to remove the natural isotopic abundances for all but one peptide (residues 278-289 of the C-subunit). Centroid determination was calculated automatically for each sample by DEX, and

checked manually for verification. To calculate the centroids, all measurable peaks, or populations, for each peptide sample were used, and the centroids were adjusted by average noise levels. The side chain exchange was determined to be 4.5% of fast exchanging side chain hydrogens [23] based on dilution factors. Side chain deuteration models were not used in the deconvolution, but their centroid values were subtracted from the centroids to show deuterium exchange of the backbone amides exclusively. The only exception was peptide m/z=1347.75 (residues 278-289), which was not deconvoluted prior to centroid analysis, due to variability in signal-noise ratio at different time points analyzed. Back exchange was found to be ~50%, so all centroid values were multiplied by a back exchange factor or 2.0 to calculate the experimental deuterium exchange levels. The average number of deuterons exchanged and standard deviations reported were determined from at three independent experiments for most peptides. Averages and standard deviations were calculated with measurements from three independent experiments for most peptides. Due to high noise in data sets for certain peptides, fewer measurements were obtained and consequently no standard deviations were calculable.

The kinetic plots of deuteration for most peptide fragments fit best to single exponential model (eq :- $D = B_{max}(1\text{-}e^{-}kt)$ where D represents the number of deuterons on the peptide at any time and B_{max} is the value at which the number of deuterons plateaus) accounting for deuterons exchanging at a rapid rate (predominantly solvent exchangeable amides). The fit was implemented in KALEIDAGRAPH 3.0 (Synergy Software, Inc., Reading, PA) [37]..

Acknowledgments

We would like to thank Drs. David Johnson, Kannan Natarajan and Cecilia Cheng for critical review of the manuscript. This work was supported by National Institutes of Health Grant GM 34921 to S.S.T.

Abbreviations and symbols

H/^{2}H exchange	hydrogen/deuterium exchange
MS	mass spectrometry
MALDI-TOF	matrix-assisted laser-desorption/ionization time-of-flight
PKA	protein kinase A
cAMP	adenosine 3′-5′-cyclic adenosine monophosphate
MOPS	3-(N-morpholino)propane sulfonic acid
cGMP	guanosine 3′-5′-cyclic guanosine monophosphate
EDTA	ethylenediaminetetraacetic acid
DTT	dithiothreitol
ATP	adenosine triphosphate
AMP-PNP	5′-adenylimidodiphosphate
TFA	trifluoroacetic acid

References

1. Francis SH, Corbin JD. Structure and function of cyclic nucleotide-dependent protein kinases. Annu Rev Physiol. 1994; 56:237–272. [PubMed: 8010741]
2. Shabb JB. Physiological substrates of cAMP-dependent protein kinase. Chem Rev. 2001; 101(8): 2381–2411. [PubMed: 11749379]

3. Taylor SS, Yang J, Wu J, Haste NM, Radzio-Andzelm E, Anand G. PKA: a portrait of protein kinase dynamics. Biochim Biophys Acta. 2004; 1697(1–2):259–269. [PubMed: 15023366]
4. Hofmann F, Beavo JA, Bechtel PJ, Krebs EG. Comparison of adenosine 3′:5′-monophosphate-dependent protein kinases from rabbit skeletal and bovine heart muscle. J Biol Chem. 1975; 250(19):7795–7801. [PubMed: 170270]
5. Canaves JM, Taylor SS. Classification and phylogenetic analysis of the cAMP-dependent protein kinase regulatory subunit family. J Mol Evol. 2002; 54(1):17–29. [PubMed: 11734894]
6. Amieux PS, McKnight GS. The essential role of RI alpha in the maintenance of regulated PKA activity. Ann N Y Acad Sci. 2002; 968:75–95. [PubMed: 12119269]
7. Cummings DE, Brandon EP, Planas JV, Motamed K, Idzerda RL, McKnight GS. Genetically lean mice result from targeted disruption of the RII beta subunit of protein kinase A. Nature. 1996; 382(6592):622–626. [PubMed: 8757131]
8. Thiele TE, Willis B, Stadler J, Reynolds JG, Bernstein IL, McKnight GS. High ethanol consumption and low sensitivity to ethanol-induced sedation in protein kinase A-mutant mice. J Neurosci. 2000; 20(10):RC75. [PubMed: 10783399]
9. Brandon EP, Logue SF, Adams MR, Qi M, Sullivan SP, Matsumoto AM, Dorsa DM, Wehner JM, McKnight GS, Idzerda RL. Defective motor behavior and neural gene expression in RIIbeta-protein kinase A mutant mice. J Neurosci. 1998; 18(10):3639–3649. [PubMed: 9570795]
10. Newhall KJ, Cummings DE, Nolan MA, McKnight GS. Deletion of the RIIbeta-subunit of protein kinase A decreases body weight and increases energy expenditure in the obese, leptin-deficient ob/ob mouse. Mol Endocrinol. 2005; 19(4):982–991. [PubMed: 15618289]
11. Huang LJ, Taylor SS. Dissecting cAMP binding domain A in the RIalpha subunit of cAMP-dependent protein kinase. Distinct subsites for recognition of cAMP and the catalytic subunit. J Biol Chem. 1998; 273(41):26739–26746. [PubMed: 9756917]
12. Ringheim GE, Taylor SS. Dissecting the domain structure of the regulatory subunit of cAMP-dependent protein kinase I and elucidating the role of MgATP. J Biol Chem. 1990; 265(9):4800–4808. [PubMed: 2156855]
13. Herberg FW, Dostmann WR, Zorn M, Davis SJ, Taylor SS. Crosstalk between domains in the regulatory subunit of cAMP-dependent protein kinase: influence of amino terminus on cAMP binding and holoenzyme formation. Biochemistry. 1994; 33 (23):7485–7494. [PubMed: 8003514]
14. Poteet-Smith CE, Shabb JB, Francis SH, Corbin JD. Identification of critical determinants for autoinhibition in the pseudosubstrate region of type I alpha cAMP-dependent protein kinase. J Biol Chem. 1997; 272(1):379–388. [PubMed: 8995272]
15. Anand GS, Hughes CA, Jones JM, Taylor SS, Komives EA. Amide H/2H exchange reveals communication between the cAMP and catalytic subunit-binding sites in the R(I)alpha subunit of protein kinase A. J Mol Biol. 2002; 323(2):377–386. [PubMed: 12381327]
16. Kim C, Xuong NH, Taylor SS. Crystal structure of a complex between the catalytic and regulatory (RIalpha) subunits of PKA. Science. 2005; 307(5710):690–696. [PubMed: 15692043]
17. Hamuro Y, Zawadzki KM, Kim JS, Stranz DD, Taylor SS, Woods VL Jr. Dynamics of cAPK type II beta activation revealed by enhanced amide H/2H exchange mass spectrometry (DXMS). J Mol Biol. 2003; 327(5):1065–1076. [PubMed: 12662931]
18. Rosen OM, Erlichman J. Reversible autophosphorylation of a cyclic 3′:5′-AMP-dependent protein kinase from bovine cardiac muscle. J Biol Chem. 1975; 250(19):7788–7794. [PubMed: 240840]
19. Herberg FW, Taylor SS. Physiological inhibitors of the catalytic subunit of cAMP-dependent protein kinase: effect of MgATP on protein-protein interactions. Biochemistry. 1993; 32(50): 14015–14022. [PubMed: 8268180]
20. Anand G, Taylor SS, Johnson DA. Cyclic-AMP and Pseudosubstrate Effects on Type-I A-Kinase Regulatory and Catalytic Subunit Binding Kinetics. Biochemistry. 2007; 46(32):9283–9291. [PubMed: 17658893]
21. Zawadzki KM, Taylor SS. cAMP-dependent protein kinase regulatory subunit type II beta: active site mutations define an isoform-specific network for allosteric signaling by cAMP. J Biol Chem. 2004; 279(8):7029–7036. [PubMed: 14625280]
22. Anand GS, Law D, Mandell JG, Snead AN, Tsigelny I, Taylor SS, Ten Eyck LF, Komives EA. Identification of the protein kinase A regulatory RIalpha-catalytic subunit interface by amide H/2H

exchange and protein docking. Proc Natl Acad Sci U S A. 2003; 100(23):13264–13269. [PubMed: 14583592]

23. Hotchko M, Anand GS, Komives EA, Ten Eyck LF. Automated extraction of backbone deuteration levels from amide H/2H mass spectrometry experiments. Protein Sci. 2006; 15(3): 583–601. [PubMed: 16501228]
24. Hughes CA, Mandell JG, Anand GS, Stock AM, Komives EA. Phosphorylation causes subtle changes in solvent accessibility at the interdomain interface of methylesterase CheB. J Mol Biol. 2001; 307(4):967–976. [PubMed: 11286548]
25. McKnight GS, Cummings DE, Amieux PS, Sikorski MA, Brandon EP, Planas JV, Motamed K, Idzerda RL. Cyclic AMP, PKA, and the physiological regulation of adiposity. Recent Prog Horm Res. 1998; 53:139–159. discussion 160–131. [PubMed: 9769707]
26. Hamuro Y, Anand GS, Kim JS, Juliano C, Stranz DD, Taylor SS, Woods VL Jr. Mapping intersubunit interactions of the regulatory subunit (RIalpha) in the type I holoenzyme of protein kinase A by amide hydrogen/deuterium exchange mass spectrometry (DXMS). J Mol Biol. 2004; 340(5):1185–1196. [PubMed: 15236976]
27. Vigil D, Blumenthal DK, Heller WT, Brown S, Canaves JM, Taylor SS, Trewhella J. Conformational differences among solution structures of the type Ialpha, IIalpha and IIbeta protein kinase A regulatory subunit homodimers: role of the linker regions. J Mol Biol. 2004; 337(5): 1183–1194. [PubMed: 15046986]
28. Cheng X, Phelps C, Taylor SS. Differential binding of cAMP-dependent protein kinase regulatory subunit isoforms Ialpha and IIbeta to the catalytic subunit. J Biol Chem. 2001; 276(6):4102–4108. [PubMed: 11110787]
29. Law D, Hotchko M, Ten Eyck L. Progress in computation and amide hydrogen exchange for prediction of protein-protein complexes. Proteins. 2005; 60(2):302–307. [PubMed: 15981246]
30. Kannan N, Haste N, Taylor SS, Neuwald AF. The hallmark of AGC kinase functional divergence is its C-terminal tail, a cis-acting regulatory module. Proc Natl Acad Sci U S A. 2007; 104(4): 1272–1277. [PubMed: 17227859]
31. Yang J, Garrod SM, Deal MS, Anand GS, Woods VL Jr, Taylor S. Allosteric network of cAMP-dependent protein kinase revealed by mutation of Tyr204 in the P+1 loop. J Mol Biol. 2005; 346(1):191–201. [PubMed: 15663937]
32. Deminoff SJ, Howard SC, Hester A, Warner S, Herman PK. Using substrate-binding variants of the cAMP-dependent protein kinase to identify novel targets and a kinase domain important for substrate interactions in *Saccharomyces cerevisiae.* Genetics. 2006; 173(4):1909–1917. [PubMed: 16751660]
33. Herberg FW, Taylor SS, Dostmann WR. Active site mutations define the pathway for the cooperative activation of cAMP-dependent protein kinase. Biochemistry. 1996; 35 (9):2934–2942. [PubMed: 8608131]
34. Viste K, Kopperud RK, Christensen AE, Doskeland SO. Substrate enhances the sensitivity of type I protein kinase a to cAMP. J Biol Chem. 2005; 280(14):13279–13284. [PubMed: 15691833]
35. Diller TC, Madhusudan, Xuong NH, Taylor SS. Molecular basis for regulatory subunit diversity in cAMP-dependent protein kinase: crystal structure of the type II beta regulatory subunit. Structure. 2001; 9(1):73–82. [PubMed: 11342137]
36. Herberg FW, Bell SM, Taylor SS. Expression of the catalytic subunit of cAMP-dependent protein kinase in Escherichia coli: multiple isozymes reflect different phosphorylation states. Protein Eng. 1993; 6(7):771–777. [PubMed: 8248101]
37. Mandell JG, Falick AM, Komives EA. Measurement of amide hydrogen exchange by MALDI-TOF mass spectrometry. Anal Chem. 1998; 70(19):3987–3995. [PubMed: 9784743]
38. Zheng J, Knighton DR, Ten Eyck LF, Karlsson R, Xuong N, Taylor SS, Sowadski JM. Crystal structure of the catalytic subunit of cAMP-dependent protein kinase complexed with MgATP and peptide inhibitor. Biochemistry. 1993; 32(9):2154–2161. [PubMed: 8443157]

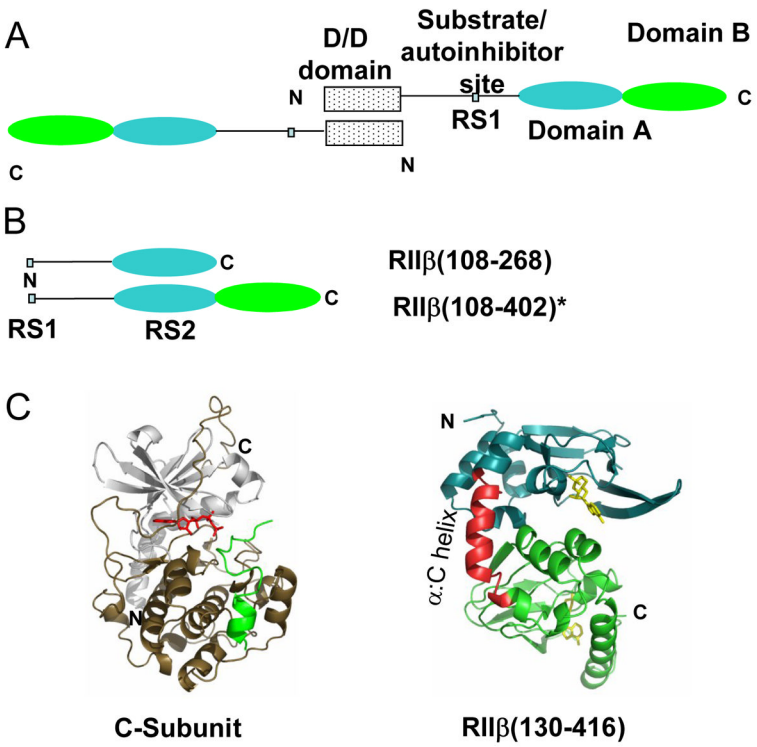

Figure 1.

Type II PKA. (*A*) Domain organization of PKA RIIβ with an N-terminal dimerization/ docking domain (D/D domain), substrate/autoinhibitor site, and two cAMP binding domains, Domain A (108–268) and Domain B (269–416). (*B*) Deletion mutants of RIIβ for probing interactions with the C-subunit, RIIβ(108–268) and RIIβ(108–402). * Increased proteolytic cleavage of C-terminal residues 403-416 during purification of the RIIβ(108–402):C holoenzyme, necessitated use of a more stable, double truncation mutant RIIβ(108–402) for studying interactions with the C-subunit. (*C*) Structures of the catalytic subunit of PKA (left) (PDB access code 1ATP) [38] and of RIIβ(right) (PDB access code 1CX4) [35]. The inhibitor peptide is green and ATP is red for C-subunit (left). In RIIβ(right), residues 108-252 are in blue, while residues 269-416 are green and the two cAMP molecules are yellow. The α:C helix (residues 253-268), a hotspot for interactions with the C-subunit is in red [17].

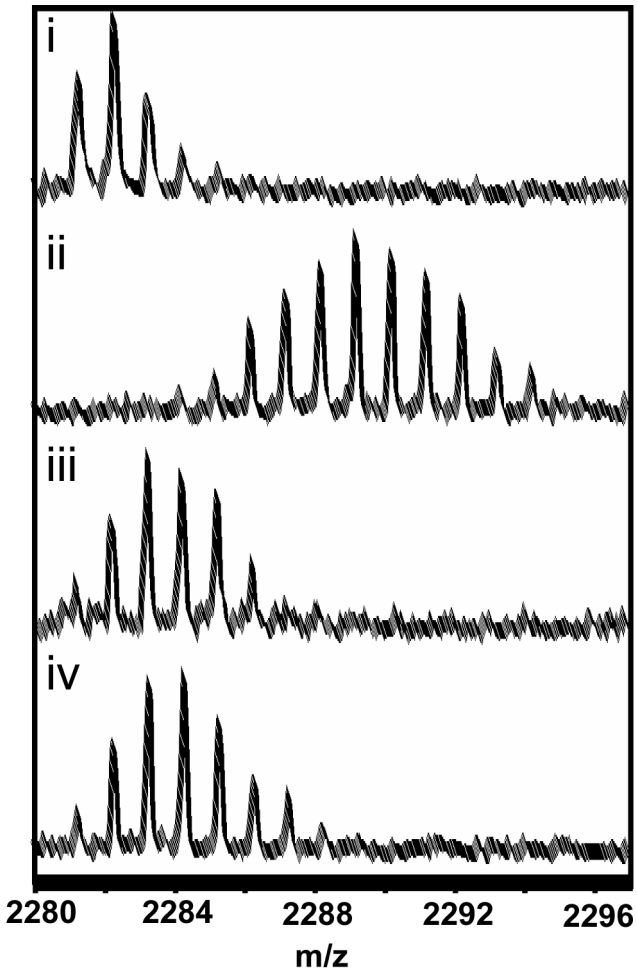

Figure 2.

MALDI-TOF spectra of one of the peptides spanning the α:C helix (residues 253-268) in RIIβ that showed decreased exchange in complexes of C-subunit with the deletion fragment, RIIβ(108–402). The spectra are expanded so as to show the isotopic distribution for the peptide of interest (*m/z* = 2281.31). i) Undeuterated sample. The higher mass peaks in the envelope are caused by naturally occurring isotopes. The isotopic envelope for the same peptide after two minutes of deuteration from:- ii) free RIIβ(residues 108-402) (iii) RIIβ(residues 108-402):C (minus Mg^{2+}ATP/Mn^{2+}AMP-PNP) and (iv) RIIβ(residues 108-402):C (plus Mn^{2+}AMP-PNP)

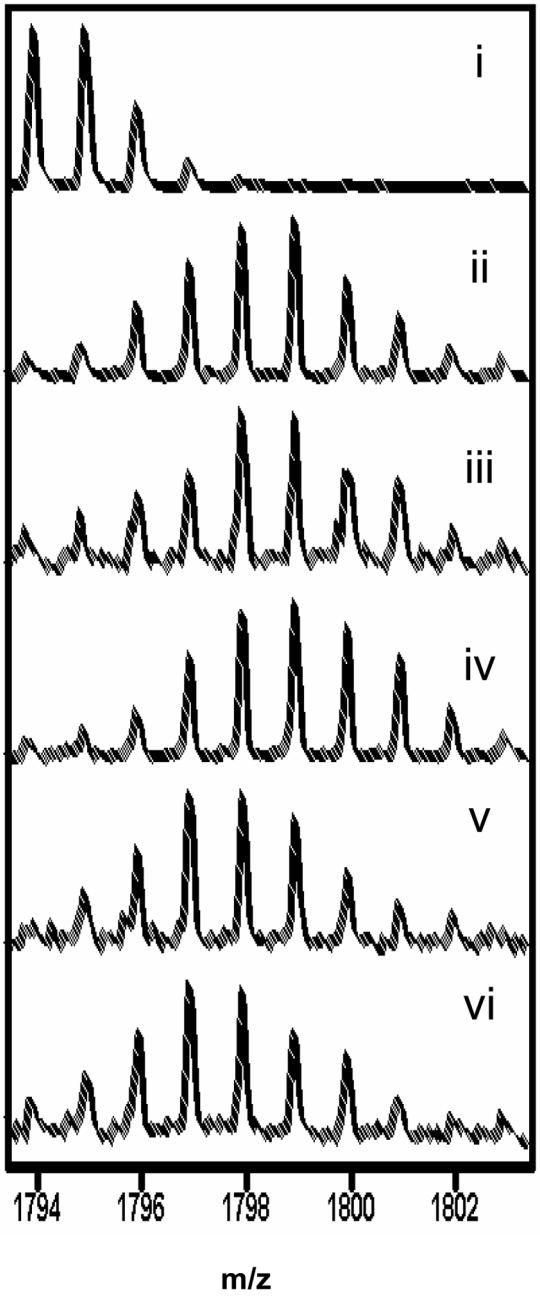

Figure 3.

MALDI-TOF spectra of one of the peptides spanning the α:G helix (residues 247-261) in the C-subunit that showed decreased exchange in complexes of C-subunit with the deletion fragment, RIIβ(108–402). The spectra are expanded so as to show the isotopic distribution for the peptide of interest (*m/z* = 1793.97). i) Undeuterated sample. The higher mass peaks in the envelope are caused by naturally occurring isotopes. The isotopic envelope for the same peptide after two minutes of deuteration from:-ii) C-subunit (minus Mg^{2+}ATP/ Mn^{2+}AMP-PNP) (iii) C-subunit (+ Mg^{2+}ATP) (iv) RIIβ(108–268):C complex + Mn^{2+}AMP-PNP, (v) RIIβ(108–402):C complex + Mn^{2+}AMP-PNP, vi) RIIβ(108–402):C complex (minus Mg^{2+}ATP/Mn^{2+}AMP-PNP).

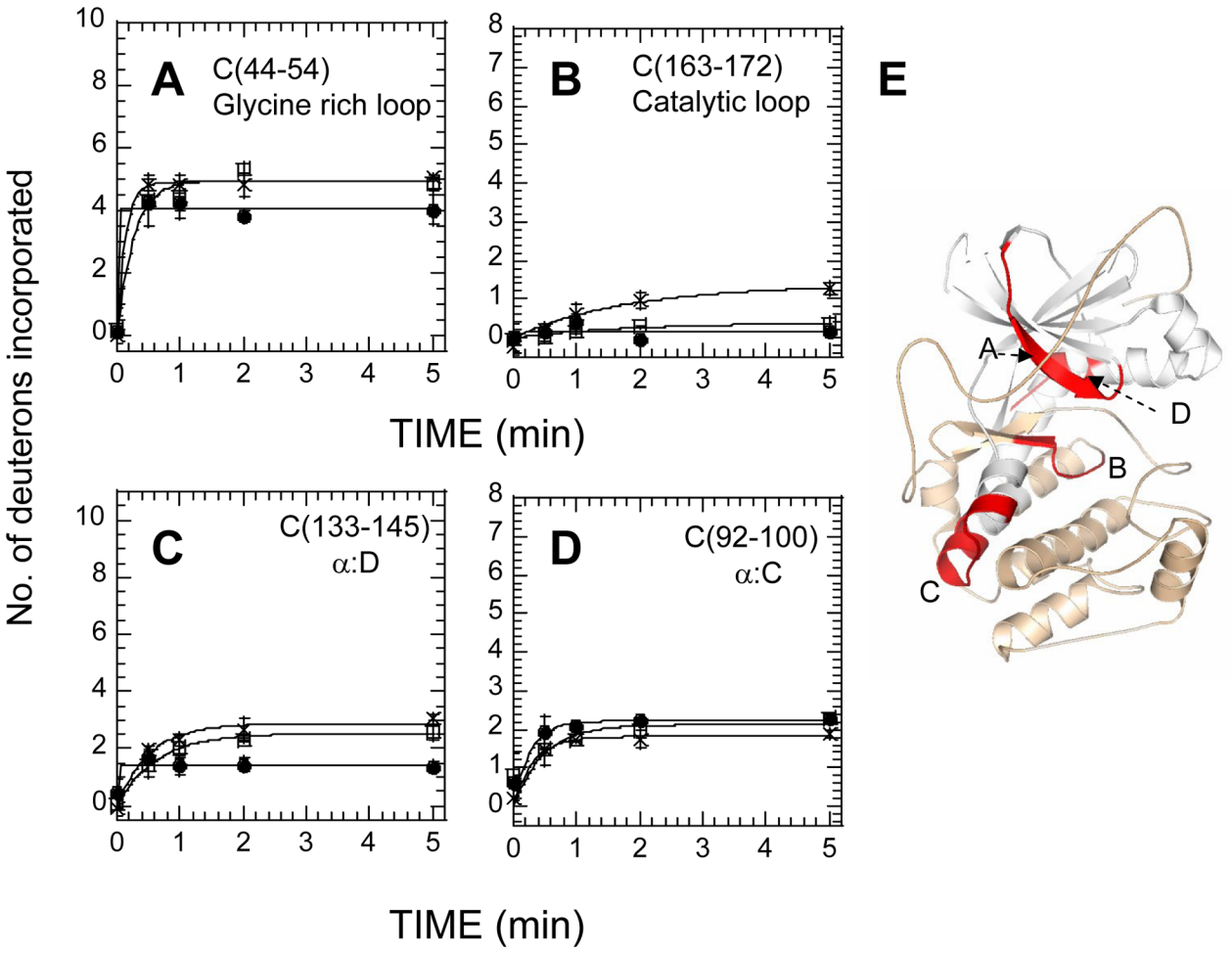

Figure 4.

Deuterium exchange in four N-terminal fragment peptides of the C subunit bound to Mg^{2+}ATP (x), bound to RIIβ(residues 108-268) and Mn^{2+}AMP-PNP (open squares)) and bound to RIIβ(residues 108-402) with Mn^{2+}AMP-PNP (filled circles)). The Y-axis scale reflects the total number of exchangeable amide hydrogens in each of the peptides analyzed. (*A*) C-subunit fragment residues 44-54 (glycine-rich loop), (*B)* C-subunit fragment residues 163-172 (catalytic loop), (C) C-subunit fragment residues 133-145 (α:D) and *D*) C-subunit fragment residues 92-100 (α:C). (*E*) Structure of the C subunit (PDB access code: 1ATP) with the N-lobe colored white and the C lobe in wheat and above four fragment peptides in red.

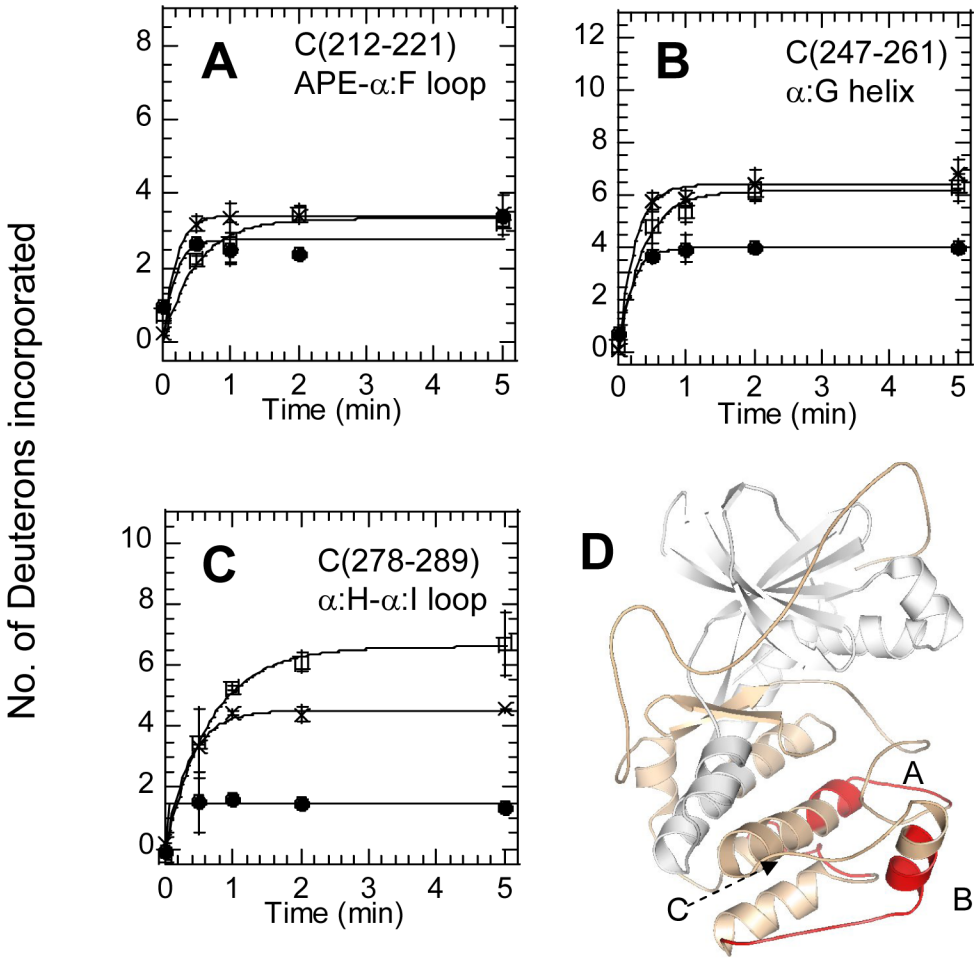

Figure 5.

Deuterium exchange in three C-lobe peptides of the C-subunit bound to Mg^{2+}ATP (x), bound to RIIβ(residues 108-268) and Mn^{2+}AMP-PNP (open squares)) and bound to RIIβ(residues 108-402) with Mn^{2+}AMP-PNP (filled circles)). (*A*) C-subunit residues 278-289 (α:Hα:I loop), (*B*) C-subunit residues 247-261, (α:G) (*C*) C-subunit residues 212-221 (APE-α:F loop). (*D*) Structure of the C subunit (PDB: 1ATP) with the N lobe colored white and the C lobe in wheat and above 3 fragment peptides in red.

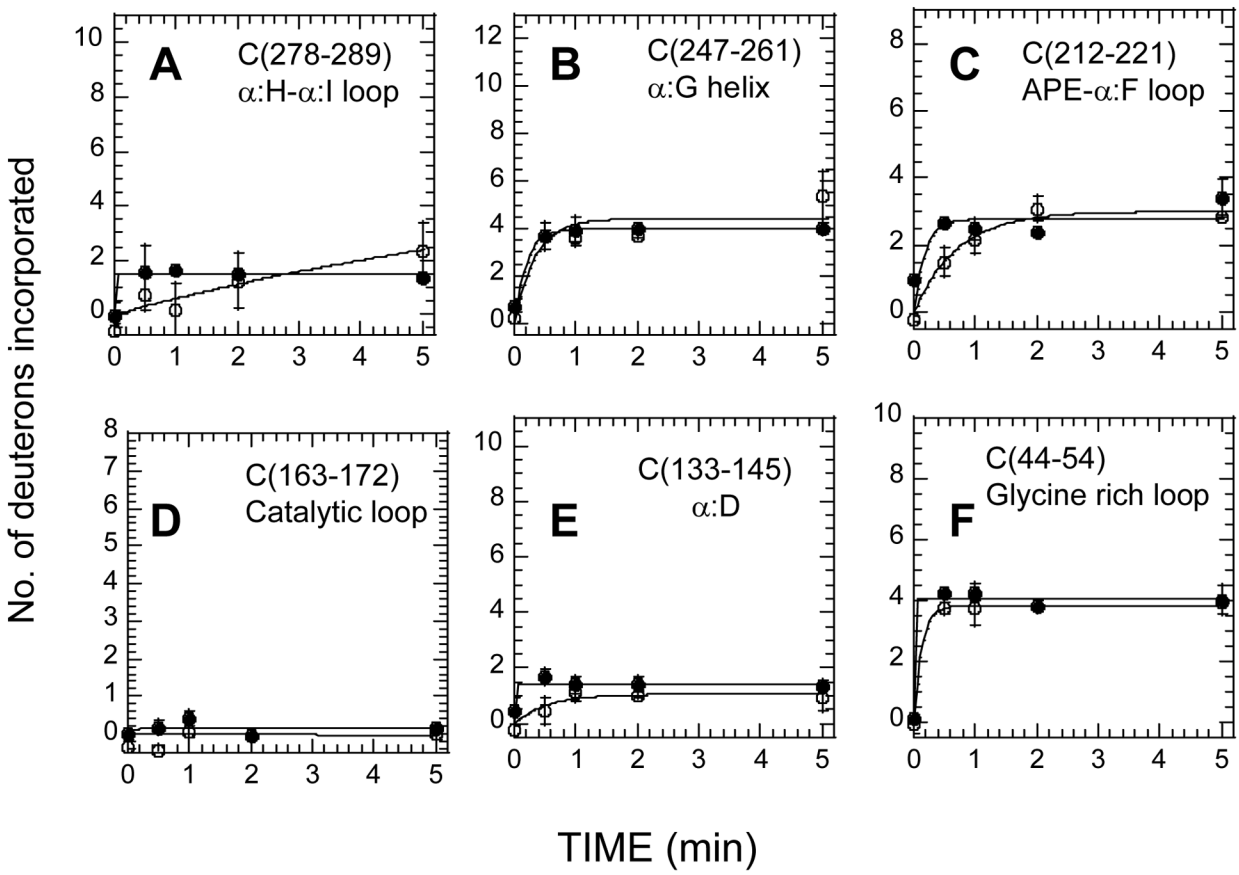

Figure 6.

(*A*)–(*F*) Deuterium exchange in six fragment peptides of the C subunit bound to RIIβ(108–402) with (filled circles)) and without Mn^{2+}AMP-PNP (open circles)). (*A*) Residues 278-289, (*B*) Residues 247-261, (*C*) Residues 212-221, (*D*) Residues 163-172, (*E*) Residues 133-145, (*F*) Residues 44-54.

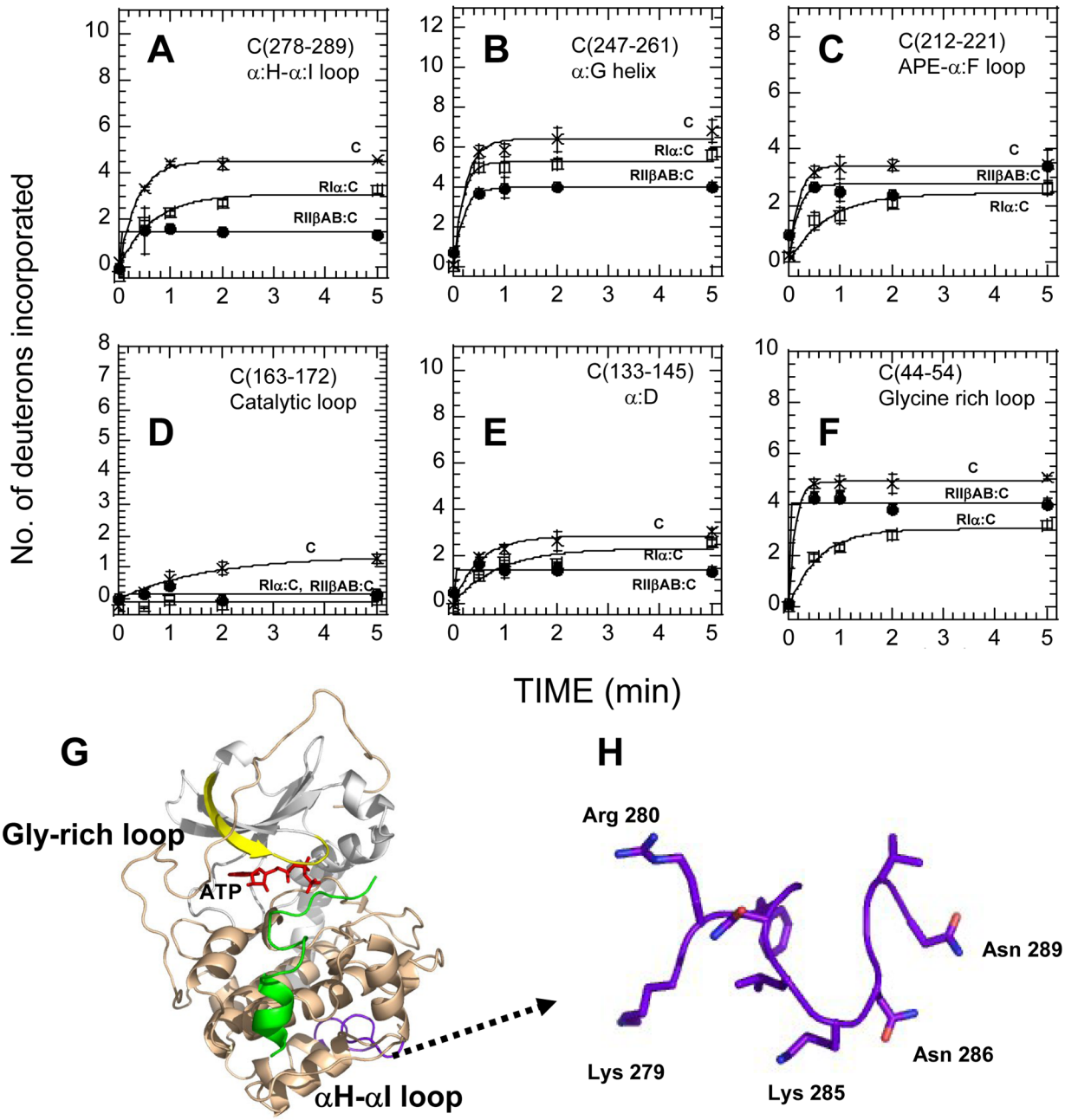

Figure 7.

(*A*)–(*F*) Deuterium exchange in six peptide fragments of the C subunit when bound to Mg^{2+}ATP (x), RIIβ(108–402) and Mn^{2+}AMP-PNP (filled circles)), and RIα; (1–379) with Mg^{2+}ATP(open squares)). (*A*) Residues 278-289, (*B*) Residues 247-261, (*C*) Residues 212-221, (*D*) Residues 163-172, (*E*) Residues 133-145, (*F*) Residues 44-54, (G) Allosteric coupling of αH-αI loop C(residues 278-289) (in purple) and the ATP binding site (Glycine-rich loop C(residues 44-54) (in yellow)), (H) Close-up of αH-αI loop C(residues 278-289) highlighting residues important for interactions between Domain B of RIIβ and the C-subunit.

Table 1

Kinetic association rate constants k_a($M^{-1}s^{-1}$) and dissociation constants k_d (s^{-1}) and affinity constants (K_D) for PKA catalytic subunit binding to RIIβ in the presence and absence of Mn^{2+}AMP-PNP, an ATP analog, by Surface Plasmon Resonance (Biacore).

Complex	k_a($M^{-1}s^{-1}$)	k_d(s^{-1})	K_D [a]	χ^2 [b]
RIIβ(108–268):C	n.d.	n.d.	n.d.	n.d.
RIIβ(108–268):C Mn^{2+}AMP-PNP	$2.0 \pm 0.3 \times 10^6$	$2.4 \pm 0.1 \times 10^{-2}$	12.0 nM	0.5
RIIβ(108–402):C	$1.5 \pm 0.2 \times 10^5$	$2.4 \pm 0.1 \times 10^{-4}$	1.6 nM	0.3
RIIβ(108–402):C Mn^{2+}AMP-PNP	$4.2 \pm 0.6 \times 10^5$	$8.4 \pm 2.6 \times 10^{-5}$	0.2 nM	0.5

[a] The K_D value is calculated from k_d and k_a, by $K_D = k_d/k_a$.

[b] A χ^2 value less than 2 can be considered a good fit. The standard errors shown have been calculated from at least two independent experiments.

Table 2

Summary of H/^{2}H exchange data for PKA catalytic subunit.

			Deuteration (2min.)				
	Fragment of PKA C-subunit (*m/z*)	**Number of amides**	**C-subunit (apo)**	**C-subunit (+Mg^{2+}ATP)**	**RIIβ(108–402):C (apo)**	**RIIβ(108–402):C (+Mn^{2+}AMP-PNP)**	**RIIβ(108–268):C (+Mn^{2+}AMP-PNP)**
C1	27-40 (1643.88)	12	7.8 ± 0.0	10.4 ± ND	-	9.8 ± 0.1	11.7 ± 0.3
C2	44-54 (1194.65)	10	6.1 ± 0.8	4.8 ± 0.4	3.8 ± 0.0	3.8 ± 0.2	5.3 ± 0.2
C3	41-54 (1584.80)	13	7.6 ± 0.0	7.2 ± 0.1	6.8 ± 0.0	5.3 ± 0.1	7.7 ± 0.2
C4	66-83(2113.23)	17	6.8 ± 0.3	5.0 ± ND	2.1 ± 0.0	5.3 ± 0.1	7.7 ± 0.2
C5	92-100 (1088.66)	8	2.3 ± 0.2	1.7 ± 0.2	1.1 ± ND	2.2 ± 0.0	2.0 ± 0.2
C6	133-145(1628.89)	11	3.7 ± 0.1	2.6 ± 0.4	1.0 ± 0.1	1.4 ± 0.2	2.3 ± 0.0
C7	164-172(1147.61)	7	1.9 ± 0.0	0.6 ± 0.0	-	-	-
C8	163-172(1260.70)	8	2.2 ± 0.3	1.0 ± 0.2	0.0 ± 0.0	0.0 ± 0.0	0.3 ± 0.0
C9	164-174(1373.78)	9	1.9 ± 0.0	2.0 ± 0.3	1.1 ± 0.1	0.4 ± 0.1	0.9 ± 0.1
C10	212-221(1167.58)	9	4.9 ± 0.8	3.4 ± 0.2	3.1 ± 0.4	2.4 ± 0.0	3.4 ± 0.2
C11	247-261(1793.97)	13	7.3 ± 0.6	6.4 ± 0.6	3.7 ± 0.1	4.0 ± 0.0	6.2 ± 0.3
C12	278-289(1347.75)	11	6.1 ± ND	4.4 ± 0.2	1.2 ± ND	1.5 ± 0.1	6.1 ± 0.3
C13	303-326(2676.45)	20	12.0 ± 0.3	11.1 ± 0.2	8.4 ± 0.3	7.5 ± ND	11.2 ± 0.3
C14	303-327(2823.52)	21	-	12.4 ± 0.2	-	-	12.6 ± 0.3
			Deuteration (2min.)				
	Sequence of RIIβ(*m/z*)	Number of amides	RIIβ(108–402)(apo)	RIIβ(108–268): (apo)	RIIβ(108–268):C(+Mn^{2+}AMP-PNP)	RIIβ(108–402):C (apo)	RIIβ(108–402):C(+Mn^{2+}AMP-PNP)
R1	226-24 (1704.97)	14	0.9 ± ND	2.5 ± 0.1	3.6 ± 0.0	0.7 ± 0.2	1.4 ± 0.0
R2	253-26 (2281.31)	17	10.7 ± ND	11.8 ± 0.1	10.8 ± 0.5	0.5 ± 0.2	0.6 ± 0.0
R3	319-33 (1790.07)	14				12.8 ± 0.1	11.2 ± 0.1
R4	339-34 (1079.58)	8	1.2 ± 0.1			2.5 ± 0.2	2.0 ± 0.1
R5	339-35 (1525.79)	12	3.1 ± 0.0			4.0 ± 0.1	4.0 ± 0.1
R6	354-37 (1824.06)	15	3.5 ± ND			4.5 ± 0.1	5.1 ± 0.1
R7	380-388 (1047.6)	7	2.7 ± ND			2.4 ± 0.0	2.3 ± 0.1

*ND: Not determined

Averages and standard deviations were calculated with measurements from three independent experiments for most peptides. Due to high noise in data sets for certain peptides, fewer measurements were obtained and consequently no standard deviations were calculable.